Influence of the strain-hardening on the bending strength and rotation capacity of welded I-section beams

1 Motivation and objectives

The most efficient use of material is one of the traditional aims of structural engineering and has recently regained much more significance due to increased demands on the life-cycle environmental costs of construction elements, for which the initial deployment of material remains the dominant factor. Owing to recent technological advances in the steel industry, structural steels with modified properties can nowadays be produced and adapted to the specific requirements of the customer, thus allowing for a more material-efficient deployment of steel if customized characteristics are used for the appropriate application. Within the framework of a research project at ETH Zurich in cooperation with a major steel producer, four steel grades with different strain-hardening behaviour were compared with each other. Possible areas of application are to be evaluated for a novel thermomechanically-rolled fine-grain steel-grade with a pronounced hardening behaviour and the potential in these areas of application is to be demonstrated. This novel TM steel with pronounced hardening is commercially termed “slim-fit steel” with designation S355M_SF. Making the potential of this and other application taylored steel grades available to practice will contribute to an optimisation of steel consumption and thus to the creation of more slender and economical steel structures.

The focus of this thesis is on the experimental and numerical investigation of the bending behaviour of welded I-section beams. In contrast to recent studies, where mostly high-strength steel has been investigated (for example: H. S. Joo et al. (2013) [1] or Schillo & Feldmann (2017) [2]), this research focusses on the hardening characteristics of the steel and its implications. A series of 4-point bending tests were conducted and used to validate numerical models. These validated simulations will be used to re-evaluate the cross-sectional classification according to Eurocode 3 [3] and the rules for the design against local buckling. It is thus aimed to make the beneficial characteristics of steel grades with pronounced hardening available to practice and thus make the use steel more economical.

2 Description of method and results

The different hardening characteristics of the four steel grades are shown by coupon tensile tests in Figure 1. The S355M_SF steel differs from the other considered steel grades (S355J2N, S460M and S355M) due to a much higher ratio between tensile and yield strength with f_u/f_y = 1.67 and the lack of a clear yield point and plateau (see Table 1).

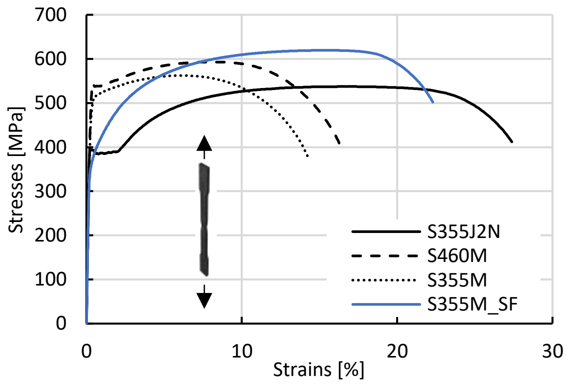

Figure 1: Stress-strain behaviour of the four steel grades

Table 1: Characteristic stress values of the four steel grades

Steel grades	f_y [MPa]	f_u [MPa]	f_u/f_y [-]
S355J2N	393	537	1.37
S460M	543	593	1.09
S355M	507	562	1.11
S355M_SF	370	619	1.67

A total of eight 4-point bending tests were carried out. The used measuring equipment and its arrangement, as well as the most important dimensions of the beams are shown in Figure 2. The beams having a flange width of 210 mm correspond to a cross-section class 1 (CSC 1) and those having a flange width of 310 mm to a cross-section class 3 (CSC 3) according to SIA 263:2013 [4] and Eurocode 1993-1-1:2005 [3].

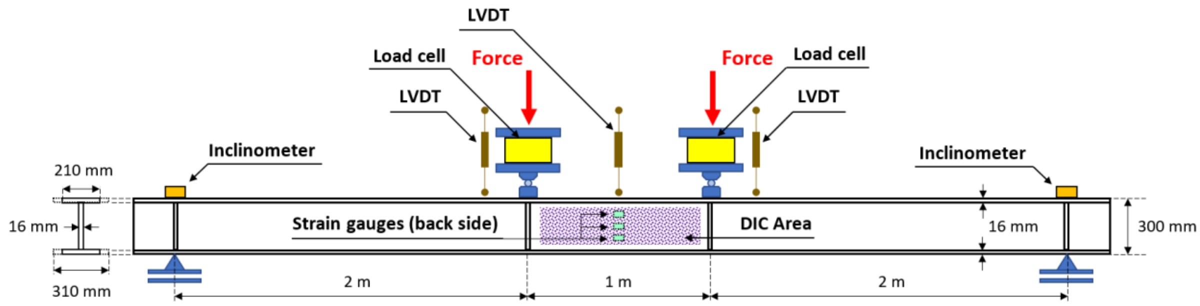

Figure 2: Dimensions of the test setup and arrangement of the measuring equipment

The eight moment-rotation curves of the four investigated steel grades are shown for the CSC 1 beams in Figure 3a and the CSC 3 beams in Figure 3b. To eliminate the influence of the different yield stresses, all axes were normalised. Figure 3a shows that the three commercially available CSC 1 beams just reach the plastic bending resistance M_{pl}. Especially the two steel grades S355M and S460M, which have a very small tensile to yield strength ratio (see Table 1), show almost no increases in the bending resistance after exceeding M_{pl}. On the other hand, the beam made of the new S355M_SF steel, reaches a maximum bending resistance that is almost 40 % above M_{pl}. As a result of its pronounced hardening behaviour, additional load-bearing capacity can be activated, and a significant increase in rotation capacity can be achieved.

Figure 3b shows the moment-rotation curves of the CSC 3 beams. Again, the behaviour of the S355M_SF beam is characterised by significantly increased load-bearing resistances and higher rotational capacity compared to the beams made of the commercially available steel grades. The experiments confirm that the pronounced hardening behaviour of the new S355M_SF leads to an increased bending resistances as well as to a bigger rotational capacity.

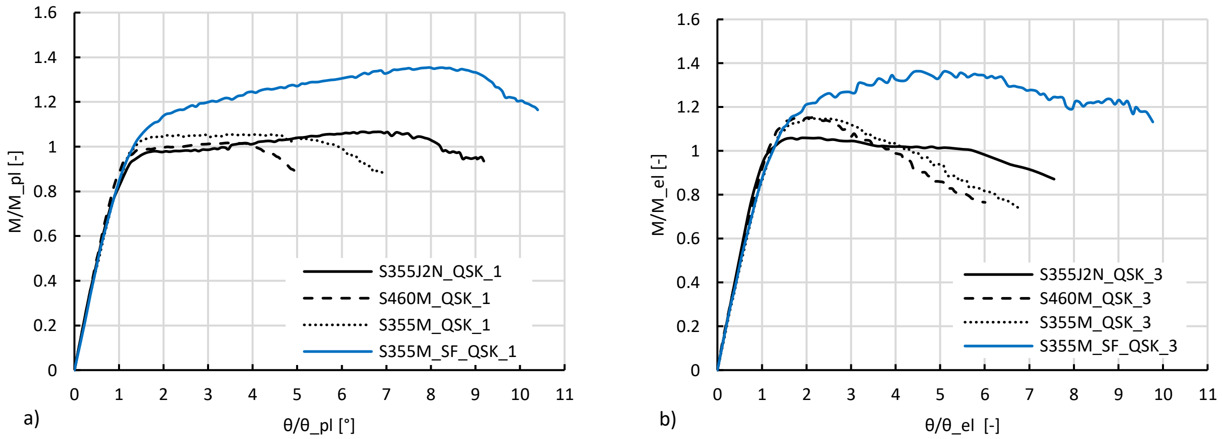

Figure 3: Moment-rotation curves with normalised axes for comparison of the steel grades: a) CSC 1 and b) CSC 3

The investigation of the stress distribution within the cross-section was carried out by evaluating the DIC measurement data in the centre field of the beams between the load application points, where a constant bending moment acts. The variation of the stresses over the section height can be seen for different experimental time points (expressed with the current rotation) in Figure 4a for the beams of CSC 1 and in Figure 4b for those of CSC 3. It can be seen clearly that the neutral axis of the CSC 3 beams shifted downwards, whereas it remains almost unchanged for the CSC 1 beams. This new equilibrium of the tensile and compressive stresses of the CSC 3 beams implies that parts of these cross-sections are withdrawing from the load due to local buckling phenomena. Using these data, an additional validation of the common assumptions of plane strain surfaces, linear elastic and constant plastic stress curves over the I-beam cross-section can be provided.

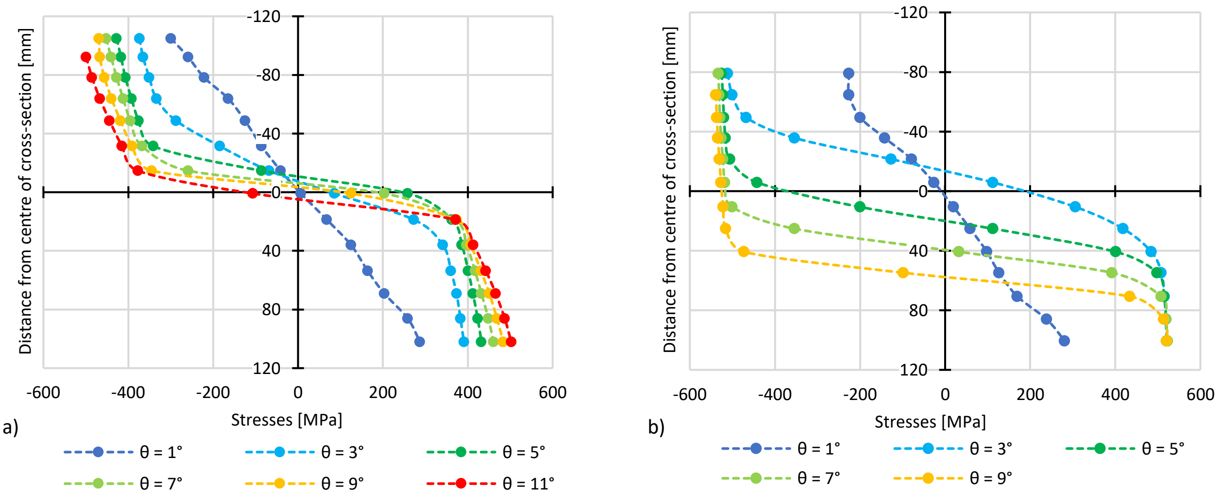

***Figure 4:** Stresses distribution along DIC height over different rotations in the experiment: a) S355M_SF_CSC_1 and b) S355M_CSC_3*

In order to gather a wider picture of the buckling behaviour of welded sections made from the S355M_SF steel, a comprehensive parametric study using numerical models was planned and is currently being continued at ETHZ. For this, numerical models were developed, using a shell-based model with S4R elements in the finite element software Abaqus [5]. The calibration of the numerical simulations on the basis of the physical experiments showed that the choice of the imperfection shape is of main, and the amplitude of this imperfection shape is of only secondary importance. Good agreements between experiments and simulation can be achieved if an imperfection shape in the form of the first buckling shape (Eigenmode 1) is assumed, and an amplitude of 1 mm (corresponding to 1/5000 of the free length and a small percentage of the width for all specimens) is used. The comparisons between experiments and numerical simulations are shown in Figure 5a for the CSC 1 and in Figure 5b for the CSC 3 beam made of S355M_SF. Due to the good agreement, it is possible to extrapolate the curves based on the numerical simulations. This makes it possible to estimate values for the rotational capacity of the two S355M_SF beams, which can be taken directly from Figure 5a and Figure 5b.

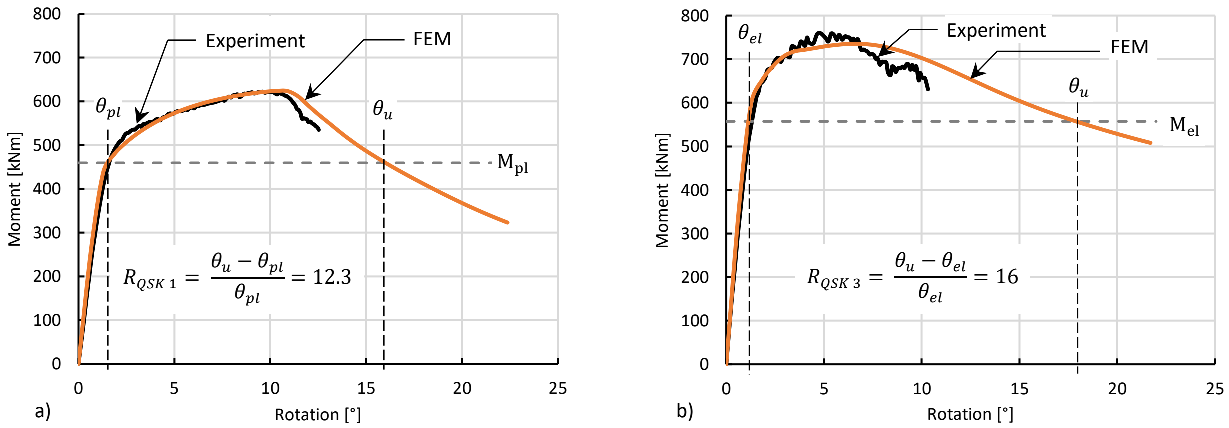

Figure 5: Moment-rotation curves from experiment and FEM-model made of S355M_SF: a) CSC 1 and b) CSC 3

The maximum bending strength and rotational capacities from the experiments and the numerical simulations are summarised in Table 2. The numbers in the brackets representing the deviations in percent from the experiment. The maximum moment resistances can be estimated with the help of the numerical simulations with only a few percent deviation. The estimation of the rotational capacity based on numerical simulations is better for the CSC 1 beams than for those of the CSC 3. This can be attributed to the fact that the correct simulation of the local buckling phenomenon of the CSC 3 beams is more difficult to capture. It can be seen that the rotational capacities of the two S355M_SF beams are much higher (up to 3 times) than the values of the standard beams. Based on the moment-rotation curves in Figure 3 and the data in Table 2, it can be confirmed that the new steel grade improves the performance of steel as a building material. The pronounced strain-hardening behaviour means that the normative bending resistances can be exceeded by almost 40 % and greater rotation capacities can be achieved.

Table 2: Experimental and numerical results of the maximum bending strength and the rotational capacity

	QSK 1				QSK 3			
	S355J2N	**S460M**	**S355M**	**S355M_SF**	**S355J2N**	**S460M**	**S355M**	**S355M_SF**
$\boldsymbol{M_{Exp}}$ $[kNm]$	**520**	**685**	**663**	622	**627**	**943**	**877**	**760**
$\boldsymbol{M_{FEM}}$ $[kNm]$	**524** (1%)	**684** (0%)	**674** (2%)	**624** (0%)	**668** (6%)	**899** (-5%)	**883** (1%)	**742** (-2%)
$\boldsymbol{R_{Exp}}$ $[-]$	**7.18**	**3**	**4.9**	N/A	**4.7**	**2.9**	**3.3**	N/A
$\boldsymbol{R_{FEM}}$ $[-]$	**7.6** (5%)	**3.3** (9%)	**4.6** (-7%)	**12.3**	**6.9** (32%)	**2.4** (-21%)	**3.6** (8%)	**16.0**

Whether the advantages of the new S355M_SF steel are sufficiently taken into account by today's standards or rather how these would need to be modified is dealt with in the final part of the thesis. For this purpose, the effective moment-rotation behaviour of numerical simulations was compared with the theoretical behaviour according to the standard. The variation of the CSC was done by increasing the flange width (b) in 50 mm steps from 160 mm to 510 mm in a FEM-based parametric study, since this unilaterally held profile segment on pure pressure becomes decisive for the classification (cf. Table 3). Figure 6 shows the effective moment-rotation curves of these fictitious beams. The graph serves to analyse the rotation capacity and the identify the limit b/t ratio after which the rotation capacity is no longer sufficient for CSC 1 requirements, yet falls into CSC 2 by achieving the plastic moment capacity. For example, the curves coloured black in Figure 6 can be said to fall within CSC 1, while the green ones fall into CSC 2. Compared to what current standards would predict, the limits for the S355M_SF steel were observed to be much less stringent, at least for the limited amount of cases that were analyses already within the framework of the thesis. First, tentative modifications to the maximum width-to-thickness ratios for the two classes were thus back-calculated and are presented here in Table 3. It is obvious that, with the help of these optimised classification ratios, more slender steel structures made of the new S355M_SF steel could be dimensioned, while still fulfilling the requirements for ductility and load-bearing resistances of the Eurocodes 3 [3].

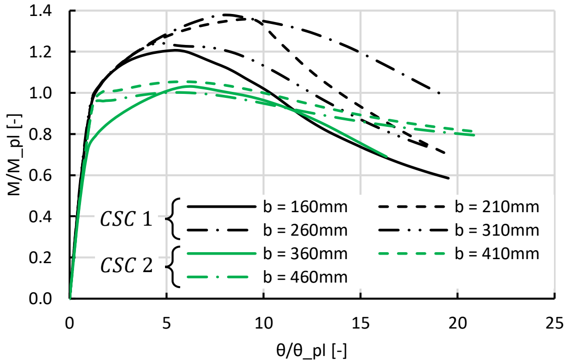

Figure 6: Effective moment-rotation curves of investigated S355M_SF beams with varied flange width (b) and new formed CSC 1 and CSC 2 groups

Table 3: Width-to-thickness ratios according to SIA 263:2013 [4] and new evaluation groups (Figure 6)

	According to SIA 263:2013 [4]	**First proposal for S355M_SF**
Stress distribution in parts (compression positive)	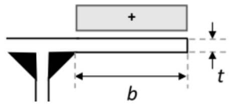	
Max. width-to-thickness ratio of CSC 1	$b/t \leq \mathbf{9}\ \varepsilon$	$b/t \leq \mathbf{11}\ \varepsilon$
Max. width-to-thickness ratio of CSC 2	$b/t \leq \mathbf{10}\ \varepsilon$	$b/t \leq \mathbf{14}\ \varepsilon$

3 Discussion of potential for application of results

The experimental testing of the four different steel grades showed that a pronounced strain-hardening behaviour of fine-grain structural steels leads to a significant increase on the bending strength and the rotational capacity of the tested I-profile beams. Quite generally, the thesis was thus able to show that developments on the metallurgical level that made the development of these steels possible are very useful to enable an improved load-bearing behaviour of steel structures. In the future, further efforts in the development of application-specific steel grades and steel characteristics should therefore be made, in order to maintain and increase the advantages of steel in key structural applications when compared to alternative materials.

Regarding more specific results of this thesis that could be directly applied to practice, it was possible to demonstrate that the imperfection shape is the central parameter for a good agreement between numerical simulation and experiment when studying the behaviour of stockier sections from CSC 3 to 1; the actual amplitude of the imperfection, as well as the patterns of residual stresses, were shown to be of secondary importance. By experimentally validating the common assumption that the choice of the first buckling eigenmode as imperfection shape provides a good approximation of the carrier behaviour, a useful guidance for applications of this type of numerical analysis in practice was provided. This generates added value for further investigations in that the number of expensive and time-consuming physical experiments can be reduced or partially replaced in favour of finite element calculations.

The re-evaluation of the section classes and maximum width-to-thickness ratios of the CSC 1 and 2 beams made of the new S355M_SF steel, based on the effective moment-rotation behaviour, was carried out on the previously validated FEM models. While the study needs to be further expanded in subsequent research work, it was possible to develop first proposals for new width-to-thickness limits for the cross-sectional classification. The proposal showed the optimisation potential that can still be achieved for the other decisive cross-section classification cases within the framework of further refined investigations. For only when the improvements from the metallurgical level can be taken into account by the codes, an increased economic and ecological use of steel in the construction industry will be achieved.

4 References

[1] H. S. Joo, J. Moon, B. H. Choi und H. E. Lee, „Rotational capacity and optimum bracing point of high strength steel I-girders," *Journal of Constructional Steel Research,* Bd. 88, pp. 79-89, 2013.

[2] N. Schillo und M. Feldmann, „The rotational capacity of beams made of high-strength steel," *Proceedings of the Institution of Civil Engineers-Structures and Buildings,* Bd. 170, Nr. 9, pp. 641-652, 2017.

[3] EN 1993-1-1:2005 + AC:2009. Eurocode 3, Design of steel structures – Part 1-1: General rules and rules for buildings.

[4] SIA 263:2013: Stahlbau, Schweizer Ingenieur- und Architektenverein, Zürich 2014.

[5] Abaqus/CAE (6.23) [Software]. (2020). Dassault Systèmes Simulia Corp. *https://www.3ds.com/de/produkte-und-services/simulia/produkte/abaqus/.*